

Effects of processing parameter on energy storage density and ferroelectric properties of lead-free bismuth sodium titanate-strontium bismuth titanate ceramics

Kamornporn Saenkam^{a,b}, Pharatree Jaita^{a,c}, Somnuk Sirisoonthorn^d, Tawee Tunkasiri^{a,e}, Gobwute Rujijangul^{a,c,e,f,*}

^a Department of Physics and Materials Science, Faculty of Science, Chiang Mai University, Chiang Mai 50200 Thailand

^b Graduate School, Chiang Mai University, Chiang Mai 50200 Thailand

^c Science and Technology Research Institute, Chiang Mai University, Chiang Mai 50200 Thailand

^d National Metal and Materials Technology Center, Thailand Science Park, Pathum Thani 12120 Thailand

^e Materials Science Research Center, Faculty of Science, Chiang Mai University, Chiang Mai 50200 Thailand

^f Research Center in Physics and Astronomy, Faculty of Science, Chiang Mai University, Chiang Mai 50200 Thailand

*Corresponding author, e-mail: rujijanagul@yahoo.com

Received 10 Nov 2020

Accepted 16 Apr 2021

ABSTRACT: In order to clarify the optimal sintering conditions, the effects of processing parameter on phase evolution, physical, microstructure, dielectric, ferroelectric, and energy storage density properties of bismuth sodium titanate-strontium bismuth titanate ceramics (or BNT-SBT) were investigated. The studied ceramics were fabricated via a conventional mixed oxide method and sintered at temperatures ranging from 1100–1175 °C under normal atmosphere for 3 h dwell time with a heating/cooling rate of 5 °C/min. The XRD data revealed that the coexisting rhombohedral and tetragonal phases were observed in all of the ceramics. With increasing sintering temperature, the cubic-rich phase was dominated; and the average grain size tended to increase. For the ceramics sintered at 1150 °C, the good density (5.74 g/cm³), dielectric ($\epsilon_{\max} = 3510$, $\tan \delta = 0.0501$, $T_{F-R} = 73.80$ °C, $T_m = 273$ °C), and ferroelectric ($P_r = 3.05$ $\mu\text{C}/\text{cm}^2$, $E_c = 7.69$ kV/cm) were obtained. In addition, the optimum sintering temperature of 1150 °C was also found to improve the energy storage density properties ($W = 0.94$ J/cm³, $\eta = 89.93\%$ at 125 °C, and $E = E_{\max}$).

KEYWORDS: sintering temperature, lead-free ceramics, dielectric and ferroelectric properties, energy storage density

INTRODUCTION

Materials with high energy storage density (W) and high energy storage efficiency (η) are desired to meet the growing requirements for compact electrics and devices [1, 2]. Among the various electrical energy storage materials, dielectric ceramics are widely studied for their excellent energy storage performance [3]. Ceramic-based dielectric capacitors have drawn growing interest due to their small volume, excellent thermal properties, good mechanical properties, fast charge-discharge speed, and high-power density [4]. Besides, large maximum polarization (P_{\max}) and low remnant polarization (P_r) in the relaxor ferroelectrics are key features for W and η in the selection of materials [5].

The bismuth sodium titanate ($\text{Bi}_{0.5}\text{Na}_{0.5}\text{TiO}_3$ or BNT) has been identified as a potential energy storage material because it has a large spontaneous polarization (P_s) over 40 $\mu\text{C}/\text{cm}^2$ [6], which originates from the hybridization of Bi 6p and O 2p orbitals [4]. However, the BNT has large P_r at ambient temperature and high coercive field ($E_c \sim 73$ kV/cm) [6, 7], which limit its energy storage density resulting in a small recoverable energy storage density (W_{rec}) and a low η values [4, 8, 9]. The BNT-based ceramics have also been widely used in the energy-storage devices because their permittivity and polarization are higher than other linear dielectrics [10]. For the sake of promoting the energy storage properties with decreasing P_r value, the modulation of BNT by other perovskite compositions was identified [9].

Strontium bismuth titanate ($\text{Sr}_{0.7}\text{Bi}_{0.2}\text{TiO}_3$ or SBT) is a relaxor ferroelectric with perovskite structure, which possesses several advantages for energy storage [11]. SBT ceramics exhibit good relaxor ferroelectric behavior and a diffused dielectric maximum in a wide range of temperatures, resulting from the Sr site vacancy and the off centered Bi^{3+} ion [11]. The SBT ceramics show relaxation behavior, which is essentially caused by the dipolar interaction [12]. Qiao et al [4] studied the energy density and thermal stability properties of relaxor ferroelectric BNT-SBT ceramics. In their study, the SBT was introduced into the BNT ceramic via a standard solid-state route to modulate its relaxation behavior and energy storage performance. With increasing SBT content, the perovskite structure of BNT transformed from a rhombohedral phase to a weakly polarized pseudo-cubic phase, and the relaxation behavior was enhanced. In particular, the dielectric breakdown strength (E_{DBS}) was improved from 120 kV/cm (of the pure BNT ceramic) to around 160 kV/cm (of the 0.6BNT-0.4SBT ceramic), which displayed a large W_{rec} of 2.20 J/cm³, implying a large potential ability of the 0.6BNT-0.4SBT ceramic in energy storage [4]. Li et al [5] also found a significant increase of W (1.5 J/cm³) and η (73%) for the BNT-SBT ergodic relaxor (ER) ceramics. The significant increase of W was due to the ceramics' low P_r and large P_{max} , which were induced by adding SBT into the $(1-x)\text{Bi}_{0.5}\text{Na}_{0.5}\text{TiO}_3 - x\text{Sr}_{0.85}\text{Bi}_{0.1}\text{TiO}_3$ ceramic. Ang and Yu [13] have also reported that the BNT-SBT relaxor ferroelectrics exhibit a very high ferroelectric polarization and a high purely electrostrictive strain. Therefore, it can be reasonably expected that the ER state, with low P_r , combined with large P_{max} , induced by SBT-doping BNT ceramics, might improve the energy-storage properties of the BNT-SBT ceramics.

According to the above study reports, it could say that the SBT plays an important role in improving the W_{rec} of BNT-based system. In the present study, we selected the BNT with excellent piezoelectric as base material, and a small amount of SBT was added as additive at the composition of 0.7BNT-0.3SBT ceramics (which showed interesting electrical properties, i.e the W) [4, 10]. Moreover, as sintering process is important for fabrication of ceramic materials [14], the effects of sintering temperatures on the densification, phase, microstructure, dielectric, ferroelectric, and W were investigated and discussed in details. It was expected that the optimum sintering condition could produce ceramics with better properties.

MATERIALS AND METHODS

The lead-free 0.7BNT-0.3SBT ceramic was prepared by the conventional mixed-oxide method. Analytical grade reagents of Bi_2O_3 , Na_2CO_3 , TiO_2 , and SrCO_3 were used as the starting raw materials. All carbonate powders were dried at 120 °C for 24 h to remove any moisture. The 0.7BNT-0.3SBT obtained was stoichiometrically weighed and mixed by ball milling in 99.9% ethanol for 24 h, and the slurry was dried in an oven. The resulted mixed powder was calcined in air atmosphere at 850 °C for 3 h dwell time. A few drops of 4 wt% polyvinyl alcohol binders were added to the mixed powder, which was then uniaxially pressed into disc pellets (10 mm in diameter and about 1.2 mm in thickness), or the ceramics, to be used as ceramic samples. The ceramics were sintered at 1100, 1125, 1150, and 1175 °C for 3 h dwell time with a heating/cooling rate of 5 °C/min in closed alumina crucibles.

Bulk density was measured with Archimedes' method. An X-ray diffractometer ((XRD, PANalytical, X' Pert Pro MPD) was used to study the phase evolution of the ceramics. A scanning electron microscope (SEM, JEOL JSM-6335F) was used to study the microstructure of the ceramics. The grain size of the ceramics was measured using the linear intercept method. Before performing the electrical measurements, all the ceramic samples had been polished into a parallel surface with 1 mm thickness. Silver paste was painted onto both sides of the pellet. Then, the samples were heated at 700 °C for 15 min to form electrodes. For electrical characterizations, dielectric properties as a function of temperature (25–500 °C) were determined using an LCR-meter (HP model 4192A) at frequencies ranging from 1 to 1000 kHz. A ferroelectric system based on Radiant Precision High Voltage Interface was used to measure the polarization-electric field (P - E) hysteresis loops at both room temperature (RT) and high temperature (HT) of 25–150 °C. A maximum electric field of 50 kV/cm and a frequency of 1 Hz were applied to each sample. P_r , P_{max} , and E_c values were determined from the hysteresis loops. By using data from ferroelectric properties, W , W_{loss} , and η values were also calculated.

RESULTS AND DISCUSSION

Densification, phase formation, and microstructure

The densification of all ceramics sintered at various sintering temperatures from 1100–1175 °C are listed in Table 1. The data clearly showed that the

Table 1 Physical, phase, microstructure, and electrical properties of 0.7BNT-0.3SBT ceramics sintered at various temperatures.

Sintering temp. (°C)	Density (g/cm ³)	<i>c/a</i>	Grain size (μm)	<i>T</i> _{FR} (°C)	<i>T</i> _m (°C)	ϵ_{\max} (@1 kHz)	$\tan \delta$ (@1 kHz)	<i>P</i> _r ^a (μC/cm ²)	<i>E</i> _c ^a (kV/cm)	<i>P</i> _r ^b (μC/cm ²)	<i>E</i> _c ^b (kV/cm)
1100	5.68	1.0100	1.28	81.12	278	3249	0.0566	2.47	5.71	1.69	0.69
1125	5.71	1.0094	1.54	74.61	275	3320	0.0396	2.84	5.77	1.14	1.75
1150	5.74	1.0084	2.02	73.80	273	3510	0.0501	3.05	7.69	0.86	3.49
1175	5.61	1.0076	2.51	70.61	271	2921	0.0388	3.62	10.9	1.30	4.48

^a Data obtained at RT and electric field of 50 kV/cm.

^b Data obtained at 125 °C and electric field of 50 kV/cm.

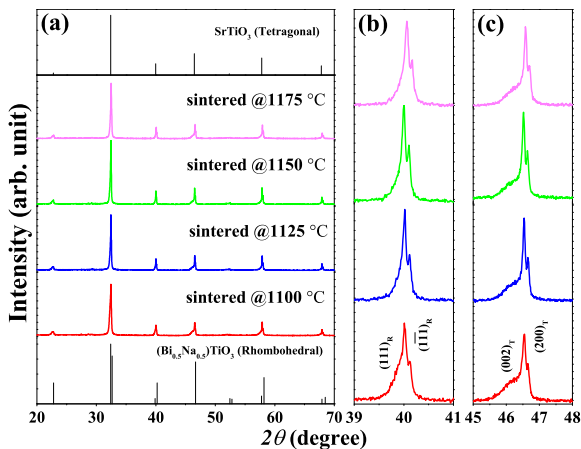


Fig. 1 X-ray diffraction patterns of 0.7BNT-0.3SBT ceramics sintered at various sintering temperatures: (a) $2\theta = 20\text{--}70^\circ$, (b) $2\theta = 39\text{--}41^\circ$, and (c) $2\theta = 45\text{--}48^\circ$.

density was improved by the increase of sintering temperature, and a maximum value of 5.74 g/cm³ was obtained for the ceramics sintered at 1150 °C. The density was slightly decreased to the minimum value of 5.61 g/cm³ when the sintering temperature increased to 1175 °C. The reason for the decrease of density value at high temperature was likely due to the evaporation of volatile alkali metal oxides and partial melting at high temperature [15]. In addition, at sintering temperatures lower than 1100 °C, the pellet ceramic samples could not form a ceramic (not dense). Besides, it was found that at high sintering temperature over 1175 °C (such as 1200 °C), the ceramic started to melt and agglomerated with the covered powders into a hard irregular shape object. Thus, the ceramics sintered at < 1100 °C and > 1175 °C were excluded from further electrical investigation.

Fig. 1(a) shows the X-ray diffraction patterns of the 0.7BNT-0.3SBT ceramics sintered at various sintering temperatures where $2\theta = 20\text{--}70^\circ$. For the analysis of phase transition process, the XRD

patterns for selected narrow angular ranges of $2\theta = 39\text{--}41^\circ$ and $2\theta = 45\text{--}48^\circ$ are presented in Fig. 1(b) and (c), respectively. Within the resolution limit of XRD, all sintered ceramics exhibited a single phase of perovskite structure and no secondary phase could be observed, indicating that SBT completely diffused into the host lattice of BNT [4]. It was possible that a solid solution between BNT and SBT was formed. This was because when the solid solution was made, Sr ions could replace Bi and Na ions, as the ionic radius of Sr ions (1.44 Å) is not much different from the radii of Bi (1.40 Å) and Na (1.39 Å) ions (percentage of the difference is 2.86–3.59%). Moreover, the solubility limit of SBT in BNT lattice was believed to be more than 30 mol% because no trace of secondary phases was detected in XRD patterns. All sintered ceramics had a mixed phase of rhombohedral and tetragonal, as evidenced by a slight splitting of rhombohedral {111} reflections at $2\theta = 39\text{--}41^\circ$ and tetragonal {200} reflections at $2\theta = 45\text{--}48^\circ$ [16]. However, sintering temperatures had slight effects on the phase evolution. With increasing sintering temperatures, the cubic-rich phase was dominated. This behavior became clearer after the calculated lattice parameters (*a* and *c*) had been analyses, which indicated a decrease in tetragonality (*c/a*) (see Table 1).

In this study, scanning electron microscope (SEM) was used to determine the morphologies of all the ceramics. The grain size of the ceramics was measured and calculated based on a mean linear interception method. SEM micrographs, with as-sintered surface mode of the 0.7BNT-0.3SBT ceramic sintered at various sintering temperatures, are shown in Fig. 2. The average grain size values are also summarized in Table 1. It could be seen that the ceramics' grains displayed well crystallized cubic-like shape with clear boundaries. The grain sizes increased with increasing sintering temperatures, from 1.28 μm for the 1100 °C ceramic to around 2.51 μm for the 1175 °C ceramic. This behavior was in good agreement with other previously reported

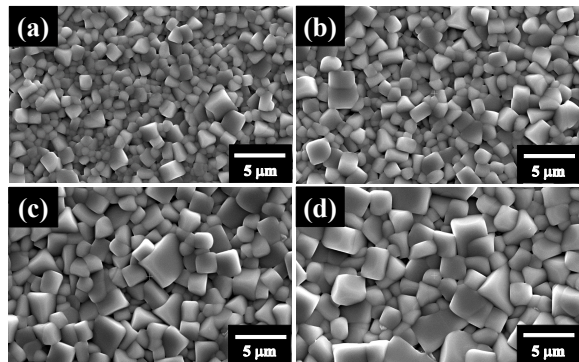


Fig. 2 SEM micrographs, with as-sintered surface mode, of 0.7BNT-0.3SBT ceramics sintered at various sintering temperatures: (a) 1100 °C, (b) 1125 °C, (c) 1150 °C, and (d) 1175 °C.

BNT-based ceramics [16, 17], and the reasons for the grain growth could be caused by a mass transfer at grain boundaries and the enhanced diffusion rate by raising sintering temperature [18].

Dielectric properties

Dielectric constant (ϵ_r) and dielectric loss ($\tan \delta$) can be used to analyse not only the ferroelectric relaxation properties, but also the phase structure changes by the anomalous points of dielectric curves [19]. Fig. 3 shows temperature dependence on ϵ_r and $\tan \delta$ of the poled 0.7BNT-0.3SBT ceramics sintered at various sintering temperatures and measured at various frequencies (from 1–1000 kHz). In BNT-based materials, two distinctive dielectric anomalies are always discerned [17]. In this study, the result showed that all the ceramic samples also existed at two dielectric peaks referred to as T_{F-R} and T_m , respectively. The first dielectric anomaly, which involved a frequency dependent dielectric permittivity, and the changes in loss tangent illustrated the relaxor ferroelectrics characteristics [20]. Normally, the lower anomaly peak is located near T_{F-R} , which is known as the ferroelectric (FE) to ergodic (ER) phase transition temperature [21]. The high temperature anomaly peak is called T_m , where the dielectric constant reaches its maximum value [22, 23]. The sintering temperature has effects on the T_{F-R} , T_m and ϵ_{max} values. Fig. 4(a) shows that the ceramics sintered 1100 °C had T_{F-R} and T_m values of 81.12 °C and 278 °C, respectively. Both T_{F-R} and T_m values decreased with increasing sintering temperatures. The downward shift of T_{F-R} with increasing sintering temperatures could be a consequence of ferroelectric order destabilization associ-

ated with the possible presence of ergodic relaxor (ER) phase in the ceramics [24]. From Fig. 4(b), the ceramic sintered at 1100 °C had maximum dielectric constant (ϵ_{max}) of 3249. The ϵ_{max} increased with increasing sintering temperatures and reached the maximum value of 3510 at 1150 °C. The value was slightly decreased when the sintering temperature was at 1175 °C. Thus, the ϵ_{max} of the ceramics could be improved by increasing the sintering temperature in this system. Normally, electrical properties of many ferroelectric materials can be influenced by many factors including grain size and density. For the grain size effect, it is known that the grain boundary is a low-permittivity region. When the grain size increases, the grain boundary decreases; thus, dielectric constant increases [25]. However, in the present study, the ϵ_{max} of the 1175 °C ceramic was less than that of the 1150 °C. Thus, the grain size might not be the main factor affecting the dielectric constant (see inset of Fig. 4(b)). Moreover, it was found that the density of the ceramics exhibited the same trend as the ϵ_{max} . Therefore, it is believed that the density should be the main factor that affects the dielectric constant. Similar observation in the BNKST ceramics was found by Tho et al [26] who reported that ϵ_{max} increased with increasing sintering temperatures, and the highest ϵ_{max} was obtained at 1100 °C, with maximum density of 5.88 g/cm³.

Ferroelectric and energy storage density analysis

The effects of sintering temperatures on polarization-electric field (P - E) hysteresis loop of the 0.7BNT-0.3SBT ceramics were investigated. Fig. 5 shows P - E hysteresis loop of the ceramic sintered at various sintering temperatures, measured at room temperature under an electric field of 50 kV/cm and a frequency of 1 Hz. The results showed that sintering temperatures had a slight influence on the ferroelectric hysteresis loop shape. However, details of the P_r and E_c are listed in Table 1. All of the ceramics exhibited a pinching in the P - E hysteresis loop at room temperature (RT), which indicated the presence of a mixture of ferroelectric (FE) and ergodic relaxor (ER) phases [27]. It should be noted that the 1150 °C exhibited a more pronounced pinched loop with low P_r . This indicated that the composition of the ceramic samples had higher amount of ER phases. At a low sintering temperature of 1100 °C, the minimum P_r of 2.47 $\mu\text{C}/\text{cm}^2$ and E_c of 5.71 kV/cm were observed. The P_r and E_c values increased with increasing sintering

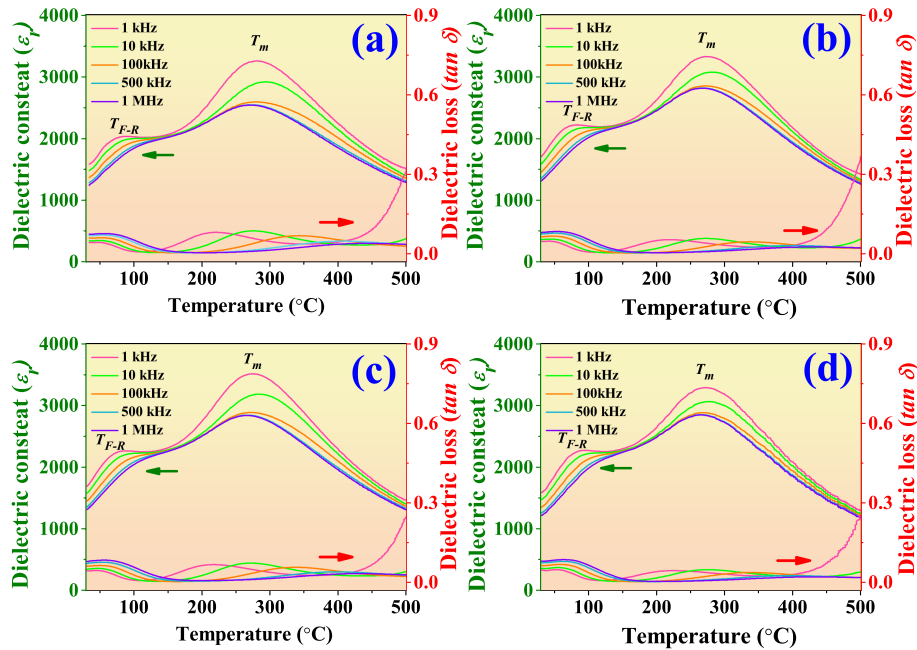


Fig. 3 Temperature dependence on dielectric constant (ϵ_r) and dielectric loss ($\tan \delta$) of poled 0.7BNT-0.3SBT ceramics sintered at various sintering temperatures, measured at various frequencies from 1–1000 kHz: (a) 1100 °C, (b) 1125 °C, (c) 1150 °C, and (d) 1175 °C.

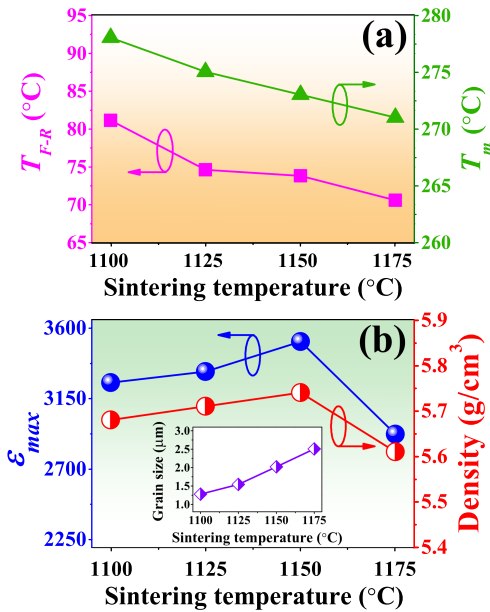


Fig. 4 Plots of (a) T_{F-R} and T_m @1 kHz as a function of sintering temperatures and (b) ϵ_{max} @1 kHz and density values as a function of sintering temperatures of 0.7BNT-0.3SBT ceramics sintered at various sintering temperatures (inset: grain sizes as a function of sintering temperatures).

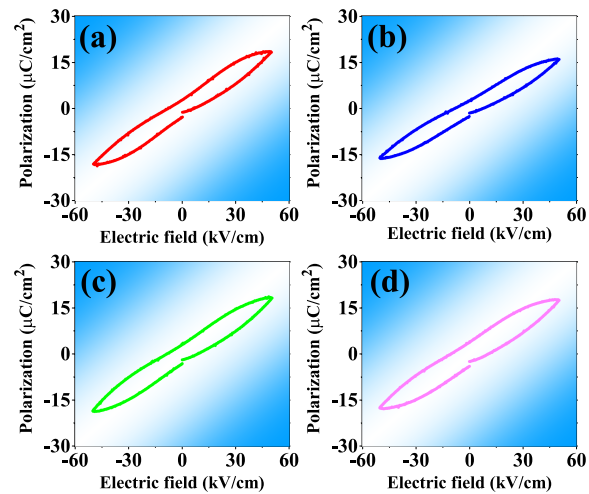


Fig. 5 Polarization-electric field ($P-E$) hysteresis loop of 0.7BNT-0.3SBT ceramics sintered at various sintering temperatures, measured at RT under an electric field of 50 kV/cm and a frequency of 1 Hz: (a) 1100 °C, (b) 1125 °C, (c) 1150 °C, and (d) 1175 °C.

temperatures and respectively showed the maximum value of 3.62 $\mu\text{C}/\text{cm}^2$ and 10.90 kV/cm for the 1175 °C ceramic. The increasing P_r value in this study could be due to the increasing grain size caused by the sintering temperature. Normally, the

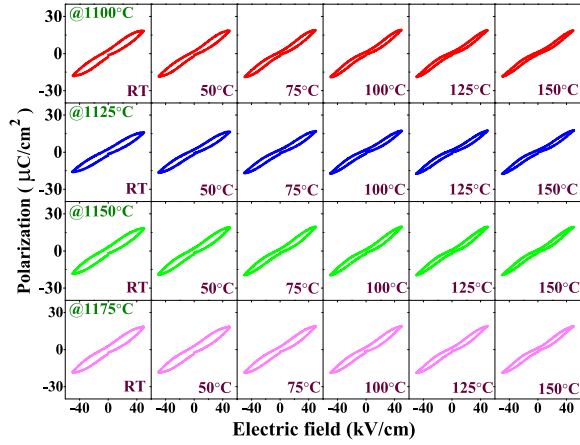


Fig. 6 Temperature dependence on polarization-electric field (P - E) hysteresis loops of 0.7BNT-0.3SBT ceramics sintered at various sintering temperatures, measured under an electric field of 50 kV/cm and a frequency of 1 Hz.

grain boundary is a low-permittivity region. That means the grain boundary has poor ferroelectricity. The number of grain boundary decreases as grain size increases, thus, P_r value increases [25]. Similar results were observed in the $\text{Ba}_{0.8}\text{Sr}_{0.2}\text{TiO}_3$ ceramics studied by Mudinepalli et al [25] who found that the P_r increased with increasing grain size and sintering temperature. Tan et al [28] also found the P_{max} and P_r slightly increased with increasing grain size for BaTiO_3 ceramic prepared by spark plasma sintering method (SPS).

Temperature dependence on polarization-electric field (P - E) hysteresis loops of the 0.7BNT-0.3SBT ceramics sintered at various sintering temperatures, measured under an electric field of 50 kV/cm and a frequency of 1 Hz are depicted in Fig. 6. All 0.7BNT-0.3SBT ceramics already exhibited ergodic relaxor (ER) characteristic at RT. When the temperature increased, the P - E hysteresis loops became more pinched, confirming that the ferroelectric to relaxor phase transition was induced by thermal activation, thus leaving an ergodic relaxor (ER) state at zero electric field [29]. The drastic decrease in both P_r and E_c values might also be related to the onset of strong ergodicity [30].

As a rule, the pinched P - E loop is always good for improving recoverable energy storage density in dielectric materials [4]. To evaluate the practicability of these ceramics for energy storage systems, the energy storage density (W) and energy storage efficiencies (η) of the studied ceramics were calculated

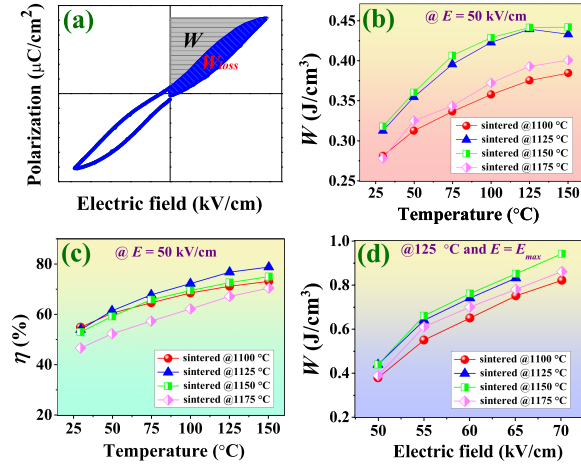


Fig. 7 Plots of (a) schematics calculation of W and W_{loss} values, (b) W as a function of temperatures ($@E = 50$ kV/cm), (c) η as a function of temperatures ($@E = 50$ kV/cm), and (d) $W @ 125^\circ\text{C}$ as a function of electric field (until breakdown strength reached) of 0.7BNT-0.3SBT ceramics sintered at various sintering temperatures.

Table 2 Energy storage properties of 0.7BNT-0.3SBT ceramics sintered at various temperatures.

Sintering temp. ($^\circ\text{C}$)	W^a (J/cm^3)	η^a (%)	W^b (J/cm^3)	η^b (%)	W^c (J/cm^3)	η^c (%)
1100	0.28	54.81	0.38	71.02	0.82	81.21
1125	0.31	53.83	0.44	76.59	0.83	84.11
1150	0.32	52.91	0.44	72.51	0.94	89.93
1175	0.28	46.61	0.39	67.03	0.86	87.90

^a Data obtained at RT and electric field of 50 kV/cm.
^b Data obtained at 125 $^\circ\text{C}$ and electric field of 50 kV/cm.
^c Data obtained at 125 $^\circ\text{C}$ and the maximum electric field.

from the P - E loops using the following equations [4, 31, 32]:

$$W = \int_{P_r}^{P_{\text{max}}} E \, dP, \quad (1)$$

$$\eta = \frac{W}{W - W_{\text{loss}}} \times 100, \quad (2)$$

where E is the electric field, P is the polarization, P_{max} is the maximum polarization, P_r is the remnant polarization, and energy loss density is denoted as W_{loss} [4, 31, 32]. In this study, the schematics calculation of W and W_{loss} values could be obtained from Fig. 7(a). Plots of W and η values as a function of the temperatures (at $E = 50$ kV/cm) of all studied ceramics are shown in Fig. 7(b) and Fig. 7(c), respectively. The related energy storage values are also summarized in Table 2. The W and η values of all ceramics increased with increasing

temperatures from RT (25 °C) to HT (150 °C) (see Fig. 7(b) and Fig. 7(c)). At the applied electric field of 50 kV/cm and at RT, the W and η values increased with increasing sintering temperatures and respectively reached the maximum values of 0.32 J/cm³ and 52.91% at 1150 °C. At the higher sintering temperature of 1175 °C, the W and η values slightly decreased.

Similarly, at the applied electric field of 50 kV/cm and at 125 °C, the W and η values of the ceramics increased with increasing sintering temperatures and respectively reached the maximum values of 0.44 J/cm³ and 71.51% at 1150 °C. In addition, plots of the W values obtained at 125 °C as a function of the electric field (until breakdown strength was reached) are shown in Fig. 7(d). At the maximum electric field and 125 °C, the ceramic sintered at 1150 °C showed the maximum values of W and η of 0.94 J/cm³ and 89.93%, respectively. Yu et al [33] have pointed out that grain size is a factor that affects the W value. However, the reason for the improvement of W of the 1150 °C ceramics in this study was likely due to the lower P_r value when compared with those of other samples (Table 1); and the lower P_r value could be a result of the higher ER phase.

Based on our results, it could be suggested that the optimum sintering temperature for preparing ceramics with high density and electrical properties, i.e. dielectric and energy storage density, was 1150 °C, and the 1150 °C ceramic could be considered as one of promising candidate materials for the production of high energy density devices.

CONCLUSION

In this study, the 0.7Bi_{0.5}Na_{0.5}TiO₃-0.3Sr_{0.7}Bi_{0.2}TiO₃, or 0.7BNT-0.3SBT, ceramics sintered at various sintering temperatures were successfully synthesized by a conventional mixed oxide method. The processing sintering temperature had a strong effect on microstructure, dielectric, ferroelectric, and energy storage density properties of the ceramics. The optimum sintering temperature for preparing ceramics with high densification and electrical performance was 1150 °C. Grain size values increased with increasing sintering temperature. The ceramic sintered at 1150 °C showed good densification (bulk density = 5.74 g/cm³), dielectric (ϵ_{\max} = 3510, $\tan \delta$ = 0.0501, T_{F-R} = 73.80 °C, T_m = 273 °C), ferroelectric (P_r = 3.05 μ C/cm², E_c = 7.69 kV/cm), and energy storage properties (W = 0.94 J/cm³, η = 89.93% at 125 °C and maximum electric field). Based on our results, the sintering temperature

for preparing ceramics with high density and high electrical and energy storage density properties was 1150 °C.

Acknowledgements: This study was supported by the Chiang Mai University and National Research Council of Thailand (NRCT). Research Center in Physics and Astronomy, Materials Science Research Center, Basic Research Fund, Global Partnership Project, Department of Physics and Materials Science, Science and Technology Research Institute, and Graduate School, Chiang Mai University are also acknowledged.

REFERENCES

1. Yang H, Yan F, Lin Y, Wang T, He L, Wang F (2017) A lead free relaxation and high energy storage efficiency ceramics for energy storage applications. *J Alloys Compd* **710**, 436–445.
2. Xu Q, Li T, Hao H, Zhang S, Wang Z, Cao M, Yao Z, Liu H (2015) Enhanced energy storage properties of NaNbO₃ modified Bi_{0.5}Na_{0.5}TiO₃ based ceramics. *J Eur Ceram Soc* **35**, 545–553.
3. Li Q, Yao Z, Ning L, Gao S, Hu B, Dong G, Fan H (2018) Enhanced energy-storage properties of (1-x)(0.7Bi_{0.5}Na_{0.5}TiO₃-0.3Bi_{0.2}Sr_{0.7}TiO₃)-xNaNbO₃ lead-free ceramics. *Ceram Int* **44**, 2782–2788.
4. Qiao X, Wu D, Zhang F, Niu M, Chen B, Zhao X, Liang P, Wei L, et al (2019) Enhanced energy density and thermal stability in relaxor ferroelectric Bi_{0.5}Na_{0.5}TiO₃-Sr_{0.7}Bi_{0.2}TiO₃ ceramics. *J Eur Ceram Soc* **39**, 4778–4784.
5. Li QN, Zhou CR, Xu JW, Yang L, Zhang X, Zeng WD, Yuan CL, Chen GH, et al (2016) Ergodic relaxor state with high energy storage performance induced by doping Sr_{0.85}Bi_{0.1}TiO₃ in Bi_{0.5}Na_{0.5}TiO₃ ceramics. *J Electron Mater* **45**, 5146–5151.
6. Jaita P, Jarupoom P (2020) Temperature dependence on structure, mechanical and electrical properties of bismuth lanthanum sodium titanate-modified lead zirconate titanate ceramics. *ScienceAsia* **46S**, 51–57.
7. Jaita P, Sanjoom R, Lertcumfu N, Malasri P, Rujijangul G, Tunkasiri T (2020) Effect of barium iron tantalate incorporation on mechanical, electrical, and magnetocapacitance properties of modified bismuth sodium potassium titanate ceramics. *ScienceAsia* **46S**, 66–73.
8. Yin J, Zhang YX, Lv X, Wu JG (2018) Ultrahigh energy-storage potential under low electric field in bismuth sodium titanate-based perovskite ferroelectrics. *J Mater Chem A* **6**, 9823–9832.
9. Qiao X, Zhang F, Wu D, Chen B, Zhao X, Peng Z, Ren X, Liang P, et al (2020) Superior comprehensive energy storage properties in Bi_{0.5}Na_{0.5}TiO₃-based relaxor ferroelectric ceramics. *Chem Eng J* **388**, ID 124158.
10. Hu B, Fan H, Ning L, Gao S, Yao Z, Li Q (2018) Enhanced energy-storage performance and dielectric

- temperature stability of $(1-x)(0.65\text{Bi}_{0.5}\text{Na}_{0.5}\text{TiO}_3 - 0.35\text{Bi}_{0.1}\text{Sr}_{0.85}\text{TiO}_3) - x\text{KNbO}_3$ ceramics. *Ceram Int* **44**, 10968–10974.
11. Zhao P, Tang B, Si F, Yang C, Li H, Zhang S (2020) Novel Ca doped $\text{Sr}_{0.7}\text{Bi}_{0.2}\text{TiO}_3$ lead-free relaxor ferroelectrics with high energy density and efficiency. *J Eur Ceram Soc* **40**, 1938–1946.
 12. Chen A, Zhi Y (2002) Dielectric relaxor and ferroelectric relaxor: Bi-doped paraelectric SrTiO_3 . *J Appl Phys* **91**, ID 1487.
 13. Ang C, Yu Z (2010) Dielectric and ferroelectric properties in $(\text{Sr}, \text{Ni}, \text{Na})\text{TiO}_3$ solid solutions. *J Appl Phys* **107**, ID 114106.
 14. Jaiban P, Jiansirisomboon S, Watcharapasorn A (2011) Densification of $\text{Bi}_{0.5}\text{Na}_{0.5}\text{ZrO}_3$ ceramic using liquid-phase sintering method. *ScienceAsia* **37**, 256–261.
 15. Moulson AJ, Herbert JM (1996) *Electroceramics*, Chapman and Hall Press, New York, USA.
 16. Dung DD, Quyet NV, Bac LH (2015) Role of sintering temperature on giant field-induced strain in lead-free $\text{Bi}_{0.5}(\text{NaK})_{0.5}\text{TiO}_3$ -based ceramics. *Ferroelectrics* **474**, 113–119.
 17. Bac DLH, Hong HS, Odkhuu D, Dung DD (2016) Effect of sintering temperature on properties of lead-free piezoelectric $0.975\text{Bi}_{0.5}(\text{Na}_{0.82}\text{K}-0.18)_{0.5}\text{TiO}_3 - 0.025\text{LiTaO}_3$ ceramics. *J Nanosci Nanotechnol* **16**, 7929–7934.
 18. Callister WD, Rethwisch DG (2003) *Materials Science and Engineering: An Introduction*, Wiley, New York, USA.
 19. Zhao N, Fan H, Ma J, Ren X, Shi Y, Zhou Y (2018) Large strain of temperature insensitive in $(1-x)(0.94\text{Bi}_{0.5}\text{Na}_{0.5}\text{TiO}_3 - 0.06\text{BaTiO}_3) - x\text{Sr}_{0.7}\text{La}_{0.2}\text{TiO}_3$ lead-free ceramics. *Ceram Int* **44**, 11331–11339.
 20. Shi J, Fan H, Liu X, Ma Y, Li Q (2015) Bi deficiencies induced high permittivity in lead-free BNBT-BST high-temperature dielectrics. *J Alloys Compd* **627**, 463–467.
 21. Ge RF, Zhao ZH, Duan SF, Kang XY, Lv YK, Yin DS, Dai Y (2017) Large electro-strain response of La^{3+} and Nb^{5+} co-doped ternary $0.85\text{Bi}_{0.5}\text{Na}_{0.5}\text{TiO}_3 - 0.11\text{Bi}_{0.5}\text{K}_{0.5}\text{TiO}_3 - 0.04\text{BaTiO}_3$ lead-free piezoelectric ceramics. *J Alloys Compd* **724**, 1000–1006.
 22. Lv YK, Duan SF, Zhao ZH, Kang XY, Ge RF, Wang H, Dai Y (2018) Enhanced electromechanical strain response in $(\text{Fe}_{0.5}\text{Nb}_{0.5})^{4+}$ -modified $\text{Bi}_{0.5}(\text{Na}_{0.8}\text{K}_{0.2})_{0.5}\text{TiO}_3$ lead-free piezoelectric ceramics. *J Mater Sci* **53**, 8059–8066.
 23. Malik RA, Hussain A, Maqbool A, Zaman A, Ahn CW, Rahman JU, Song TK, Kim WJ, et al (2015) Temperature-insensitive high strain in lead-free $\text{Bi}_{0.5}(\text{Na}_{0.84}\text{K}_{0.16})_{0.5}\text{TiO}_3 - 0.04\text{SrTiO}_3$ ceramics for actuator applications. *J Am Ceram Soc* **98**, 3842–3848.
 24. Hao J, Xu Z, Chu R, Li W, Fu P, Du J, Li G (2016) Structure evolution and electrostrictive properties in $(\text{Bi}_{0.5}\text{Na}_{0.5})_{0.94}\text{Ba}_{0.06}\text{TiO}_3 - \text{M}_2\text{O}_5$ ($\text{M} = \text{Nb}, \text{Ta}, \text{Sb}$) lead-free piezoceramics. *J Eur Ceram Soc* **36**, 4003–4014.
 25. Mudinepalli VR, Feng L, Lin WC, Murty BS (2015) Effect of grain size on dielectric and ferroelectric properties of nanostructured $\text{Ba}_{0.8}\text{Sr}_{0.2}\text{TiO}_3$ ceramics. *J Adv Ceram* **4**, 46–53.
 26. Tho NT, Vuong LD (2020) Effect of sintering temperature on the dielectric, ferroelectric and energy storage properties of SnO_2 -doped $\text{Bi}_{0.5}(\text{Na}_{0.8}\text{K}_{0.2})_{0.5}\text{TiO}_3$ lead-free ceramics. *J Adv Ceram* **4**, ID 2050011.
 27. Dinh TH, Kang JK, Lee JS, Khansur NH, Daniels J, Lee HY, Yao FZ, Wang K, et al (2016) Nanoscale ferroelectric/relaxor composites: Origin of large strain in lead-free Bi-based incipient piezoelectric ceramics. *J Euro Ceram Soc* **36**, 3401–3407.
 28. Tan Y, Zhang J, Wu Y, Wang C, Koval V, Shi B, Ye H, McKinnon R, et al (2015) Unfolding grain size effects in barium titanate ferroelectric ceramics. *Sci Rep* **5**, ID 9953.
 29. Wang K, Hussain A, Jo W, Rödel J (2012) Temperature-dependent properties of $(\text{Bi}_{1/2}\text{Na}_{1/2})\text{TiO}_3 - (\text{Bi}_{1/2}\text{K}_{1/2})\text{TiO}_3 - \text{SrTiO}_3$ lead-free piezoceramics. *J Am Ceram Soc* **95**, 2241–2247.
 30. Malik RA, Hussain A, Maqbool A, Zaman A, Song TK, Kim WJ, Kim MH (2016) Giant strain, thermally-stable high energy storage properties and structural evolution of Bi-based lead-free piezoceramics. *J Alloys Compd* **682**, 302–310.
 31. Zhao Y, Xu J, Yang L, Zhou C, Lu X, Yuan C, Li Q, Chen G, et al (2016) High energy storage property and breakdown strength of $\text{Bi}_{0.5}(\text{Na}_{0.82}\text{K}_{0.18})_{0.5}\text{TiO}_3$ ceramics modified by $(\text{Al}_{0.5}\text{Nb}_{0.5})^{4+}$ complexion. *J Alloys Compd* **666**, 209–216.
 32. Hu B, Fan H, Ning L, Wen Y, Wang C (2018) High energy storage performance of $[(\text{Bi}_{0.5}\text{Na}_{0.5})_{0.94}\text{Ba}_{0.06}]_{0.97}\text{La}_{0.0}\text{Ti}_{1-x}(\text{Al}_{0.5}\text{Nb}_{0.5})_x\text{O}_3$ ceramics with enhanced dielectric breakdown strength. *Ceram Int* **44**, 15160–15166.
 33. Yu Z, Zeng J, Zheng L, Rousseau A, Li G, Kassi A (2021) Microstructure effects on the energy storage density in BiFeO_3 -based ferroelectric ceramics. *Ceram Int* **47**, 12735–12741.